

10.6

The Dynamics of Drainage Flows Developed on a Low Angle Slope in a Large Valley Sharon Zhong¹ and C. David Whiteman²

¹Department of Geosciences, University of Houston, Houston, TX

²Pacific Northwest National Laboratory, Richland, Washington

1. INTRODUCTION

Most mountain slopes experience nocturnal drainage flows on clear nights with weak ambient winds. The characteristics of the drainage flows, however, vary widely depending on several factors including the angle, length, orientation, and vegetation cover of the slopes as well as ambient atmospheric conditions. These drainage flows can be important for atmospheric transport and dispersion within mountain valleys. In basins and valleys that are not well ventilated, the nocturnal drainage flows are known to produce cold air pools that can lead to persistent air pollution episodes and hazardous weather conditions (Whiteman et al. 2001). Nocturnal drainage flows have been extensively studied with analytical solutions (Manins and Sawford 1979; Mahrt 1982), numerical models (McNider and Pielke 1984) and field observations (Horst and Doran 1986). Majority of the drainage flow studies, however, have been concentrated on relatively steep slopes either on a side of isolated mountains, or within a deep valley.

A recent observational study conducted over a low angle slope in a large valley revealed some interesting features of nocturnal drainage flows and how they interact with ambient atmospheric stability built up in the valley. This paper presents results from numerical simulations of the observed nocturnal drainage flow development aimed at understanding the forcing mechanisms of the drainage flows developed over low-angle slopes in a large valley.

2. OBSERVATIONS

The slope flow experiment was conducted as part of the Vertical Transport and MiXing (VTMX, Doran et al. 2002) field campaign that took place in Oct. of 2000 in the Salt Lake Valley. During 8 nights with clear skies and weak ambient winds, tethersondes were operated concurrently at four locations separated by 1-km intervals along a smooth, uniform, low-angle (1.6°) slope at the foot of the Oquirrh Mountains to measure wind, temperature, and humidity from surface to over 400 m above ground at approximately 30 minute intervals.

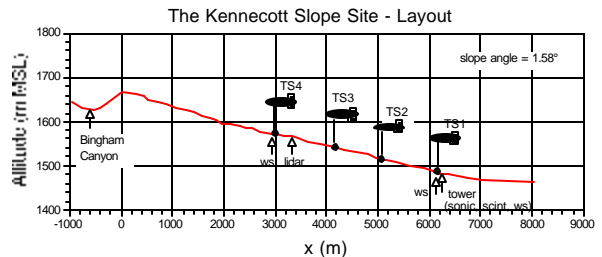


Figure 1. Topographic cross section of the slope showing the four tethered sonde sites.

On each of the 8 nights, well-developed drainage flows were observed by the tethersondes. Despite the very low slope angle, drainage flows developed were deeper and stronger than those reported previously on low-angle slopes by other investigators (Mahrt 1982). The drainage flow depth reached approximately 150 m AGL and the strength reached 5-6 m s⁻¹ at the 15-m height of the jet maximum. The temperature deficit over the slope reached 7°C at 25 m AGL, a comparable or slightly higher deficit than reported by others. The slope flows that were well-developed in the early evening often became weak and intermittent in the middle of the night as a valley inversion built up to the altitude of the slope flow sites. Over the course of the 8 nights investigated, the drainage

Corresponding author's address: Dr. Sharon Zhong,
U. of Houston, 4800 Calhoun Rd. Houston, TX 77204-
5007. szhong@uh.edu

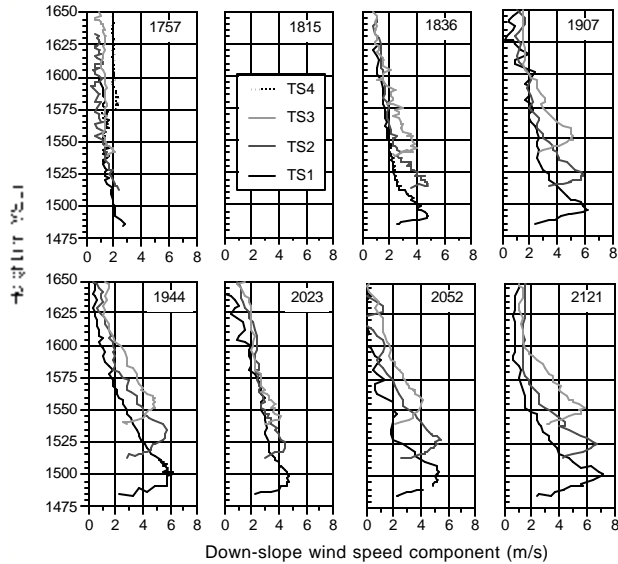


Fig. 2 Observed downslope flow component at tethered sites TS3, TS2, and TS1 on the evening of Oct. 2.

flow was often strongly affected by the larger-scale flows above the slope.

3. MODELING

The Regional Atmospheric Modeling System (RAMS; Pielke et al. 1992) was used for the model simulations. A two-dimensional terrain cross section similar to the actual slope shown in Fig.1 was used. The simulations employed two nested grids: an inner grid with 250 m grid spacing over the slope and an outer grid with 1000 m grid spacing which extends from the slope to a flat plan at the bottom. In the vertical, 7 grid points were placed in the lowest 15 m above surface (at 1, 3, 5, 7, 9, 11, 14 m) and another 8 between 15 to 50 m. The vertical grid is stretched to the model top of 9 km where the grid spacing increased to 1000 m.

4. RESULTS

A comparison of simulated and observed profiles of downslope wind components and potential temperatures are shown in Fig. 3a for the evening of Oct. 2. Similar to the observation, the simulation predicted an increase in drainage wind speed in the downslope direction. The peak wind speed increased about 1 m s^{-1} from TS3 to TS1 in the simulation, which was slightly smaller than the observed speed increase between the two sites. The simulated downslope jet profiles were slightly broader and weaker

than the observed and the height of the downslope wind maximum is slightly higher in the simulation. The simulated temperature profiles also compared reasonably well with the observed (not shown). The observed temperature decreased slightly along the downslope direction from TS3 to TS1, a feature well captured by the simulation. A strong inversion of more than $7 \text{ }^\circ\text{C}$ developed from the surface to over 50 m. The modeled inversion layer was somewhat deeper than the observed and, as a result, the strength of the inversion was weaker.

Comparisons are also shown for the evening of Oct. 8 when the ambient stability is stronger (Fig. 3b). Stronger ambient stability resulted in weaker downslope flows with maximum speed ranging between $4\text{-}5 \text{ m s}^{-1}$ compared to $5\text{-}7 \text{ m s}^{-1}$ on Oct. 2 when the ambient environment was near neutral. The heights of the wind maximum and the depths of the drainage flows appeared to be less sensitive to ambient stability as they remained similar on both evenings. The model successfully reproduced the observed difference in the temperature and wind between the two nights.

To help understand the driving forces for the unusually strong downslope flows, we carried out an analysis of the model momentum equation for the downslope wind component:

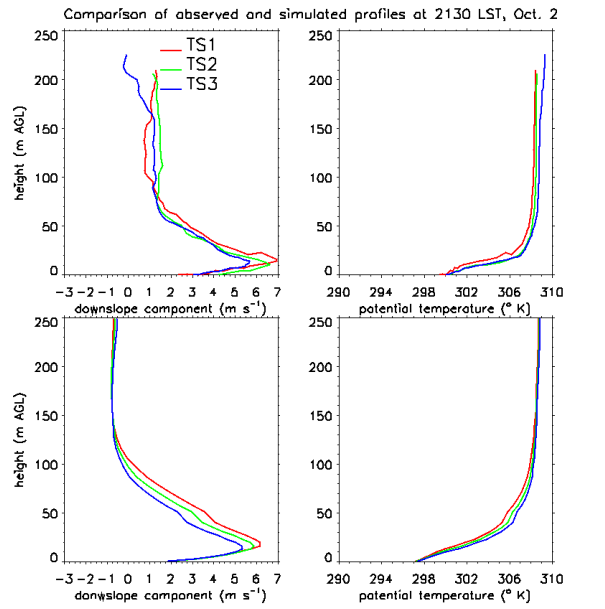


Fig. 3a. Comparison of observed (top) and simulated (bottom) downslope wind speed and temperature profiles at 2130 LST, Oct. 2.

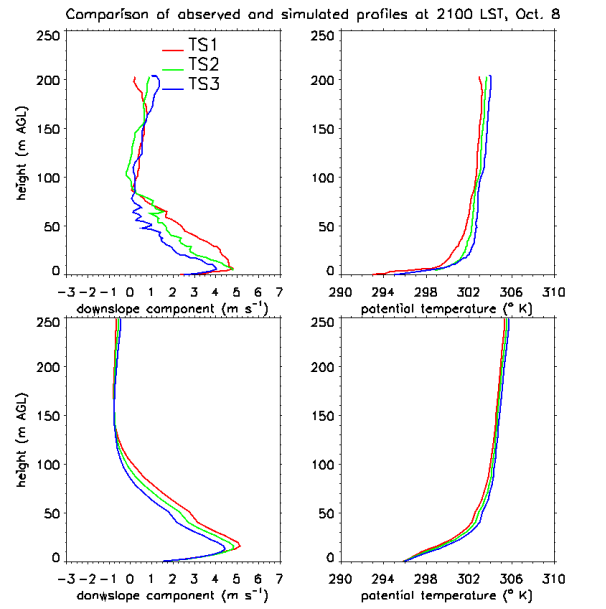


Fig. 3b. Comparison of observed (top) and simulated (bottom) downslope wind speed and temperature profiles at 2100 LST, Oct. 8.

$$\underbrace{\frac{\partial u_s}{\partial t}}_{\text{Storage}} = -\underbrace{u \frac{\partial u_s}{\partial x}}_{\text{advection}} - \underbrace{w \frac{\partial u_s}{\partial z}}_{\text{advection}} - \underbrace{\frac{1}{r} \frac{\partial p'}{\partial s}}_{\text{pressure gradient}} + \underbrace{\frac{\partial}{\partial z} \left(K \frac{\partial u}{\partial z} \right)}_{\text{diffusion}} \cos \alpha + \underbrace{g \frac{q'}{q_0}}_{\text{buoyancy}} \sin \alpha$$

which indicates that the change of downslope wind component is caused by horizontal and vertical advection of downslope wind, changes of perturbation pressure in the downslope direction, turbulent diffusion, and buoyancy.

The individual forcing terms averaged over a two hour period between 2000 and 2200 LST are shown in Fig. 4 for both cases. Despite the small slope angle of 1.6°, buoyancy force was the dominant force for the development of the downslope flows. As expected, turbulent diffusion retard the flow. The along-slope advection and pressure gradient also acted to retard the flow. Near the surface in the lowest 20 m, turbulent diffusion dominated the three negative terms. Near the jet height, the advection was the largest. It is interesting to note that pressure gradient force was previously considered negligible for uniform slopes, i.e., slopes with uniform slope angle and land surface characteristics. But as shown in Fig.4,

although the smallest among the three negative terms, along-slope pressure gradient force was not negligible. In fact, above the level of the maximum drainage flow, turbulent diffusion became very small and the pressure gradient became significant in the forcing balance. This pressure gradient force was produced, despite the uniform slope surface, when the slope flow layer gradually deepened towards the downslope direction. A comparison between the two evenings revealed that the buoyancy force was clearly larger for Oct. 2 than Oct. 8. Therefore, the result of stronger ambient stability was weaker buoyancy which, in term, led to a weaker drainage flow jet.

Similar budget analysis was done for model's heat budget and the terms in the heat budget equation are shown in Fig. 5 for the same time period as in Fig. 4. As expected, turbulent mixing helped to cool the slope flow layer by mixing air from the surface that was cooled by the radiation loss. In contrary to the common believe that a cold air advection is normally associated with downslope wind, the advective

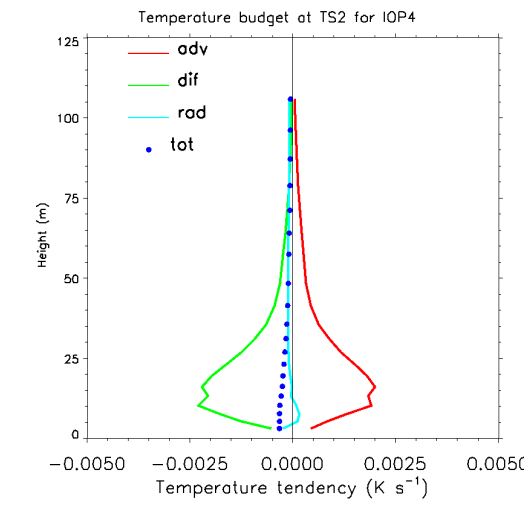
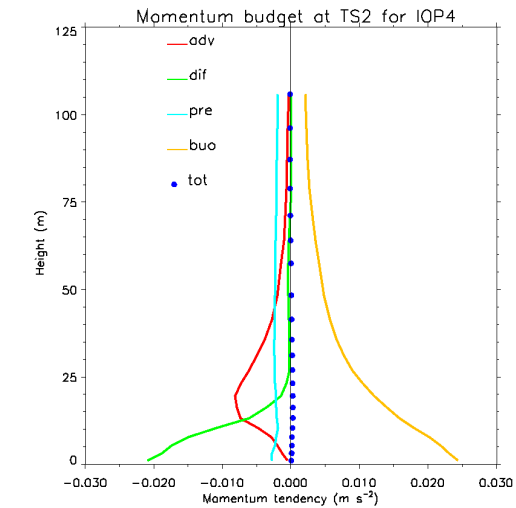
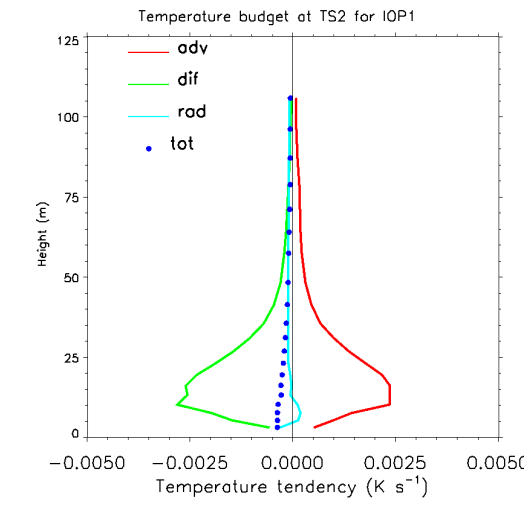
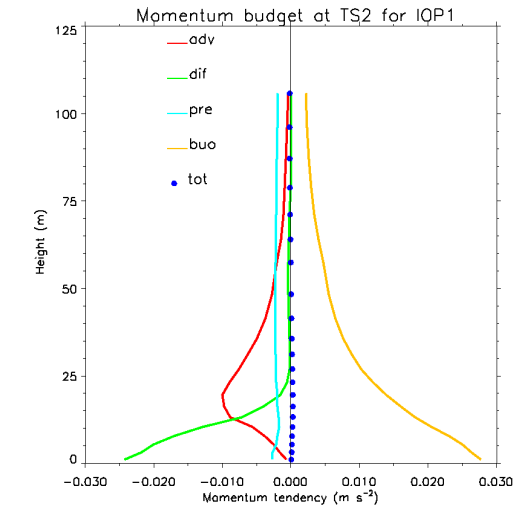


Fig. 4. Momentum budget averaged between 2000 and 2200 LST for Oct. 2 (top) and Oct. 8 (bottom).

Fig. 5. Heat budget averaged between 2000-2200 LST for Oct. 2 (top) and Oct. 8 (bottom).

term is positive that tends to balance the negative turbulent diffusion, suggesting a warm advection by downslope flow. This controversy can be explained as follows: Although downslope flow developed when air near the slope surface cools more than the air away from the slope at the *same elevation*, the sinking air is actually *warmer* than the air down the slope under the condition of temperature inversion. Therefore, as the air flowing down the slope, it brings down air that is warmer than the air adjacent to the slope at a downslope location. Despite this, air draining down the slope is generally colder than the ambient air away from the slope. This cold air flow, once reaching the

bottom of a valley or a basin, may accumulate to form a cold air pool. The development of cold air pool can affect ambient stability and winds which, in term, may affect the evolution of downslope flows.

The effect of ambient stability built up in the valley on the evolution of drainage flow is examined by a simulation using a terrain cross section shown in Fig. 6 that includes a valley between two mountains with a small (1.6°) and a large (13°) slope angles. Figure 6 shows the time variation of the maximum drainage wind speed, the depth of the drainage flow, and the mass and momentum fluxes from the simulation of

Oct. 2 at a point on each side of the four slopes near the bottom of the slopes. The drainage flows and the associated fluxes are weaker over the slopes inside the valley than those outside for both low and high angle slopes. This suggests that the accumulation of the cold air and the strengthening of the temperature inversion in the valley tend to reduce the downslope flows and the associated fluxes, which was consistent with the conclusion about the role of ambient stability when compare observations and simulations between Oct. 2 and Oct. 8. While outside the valley, the slope flows and the associated fluxes showed a steady increase during the course of the night, inside the valley the maximum speed and, to some degree, the fluxes exhibited some oscillations. Over the steep slope on the valley side, the downslope jet increased in the first few hours, started to decrease rapidly after 1000 MST, and essentially ceased after midnight. A comparison of the properties of the downslope flows developed over the shallow slope with those over the steep slope indicates that the jet speeds were higher when the slope angle is low regardless whether the slope is inside or outside the valley. The deepest downslope flow, however, occurred over the steep slopes outside the valley, which leads to largest mass flux among the four slopes.

5. ON GOING AND FUTURE WORK

More two-dimensional simulations are being carried out to investigate the sensitivity of downslope flows to ambient stability and wind, speed and direction using data from other nights. Three-dimensional simulations will be performed to examine the interaction of

downslope flows and valley circulations and determine the contribution of downslope mass flux to the buildup of cold air pool in the valley.

Acknowledgement: The authors would like to thank all the individuals who participated in the slope flow experiment, including Roland Mayer, Johanna Whiteman, Xindi Bian, Thomas Haiden, and Greg Poulos and number of students from University of Utah. The project was supported by DOE Office of Biological and Environmental Research Environmental Meteorology Program

REFERENCES

- Doran, J. C., J. D. Fast, and J. Horel, 2002: The VTMX 2000 Campaign. *Bull. Amer. Meteor. Soc.*, **83**,1233-1247.
- Doran, J. C., and T. W. Horst, 1981: Velocity and temperature oscillations in drainage winds. *J. Appl. Meteor.*, **20**, 362-364.
- Mahrt, L., 1982: Momentum balance of gravity flows. *J. Atmos. Sci.*, **39**, 2701-2711
- Manins, P. C., and B. L. Sawford, 1979a: A model of katabatic winds. *J. Atmos. Sci.*, **36**, 619-630
- McNider, R. T., and R. A. Pielke, 1984: Numerical simulation of slope and mountain flows. *J. Climate and Appl. Meteor.*, **23**, 1441-1453.
- Pielke, R. A., and co-authors, 1992: A comprehensive meteorological modeling system – RAMS. *J. Meteor. Atmos. Phys.*, **49**, 69-91
- Whiteman, C. D., S. Zhong, W. J. Shaw, J. M. Hubbe, and X. Bian, 2001: Cold pools in the Columbia Basin. *Weather and Forecasting*, **16**, 432-447.

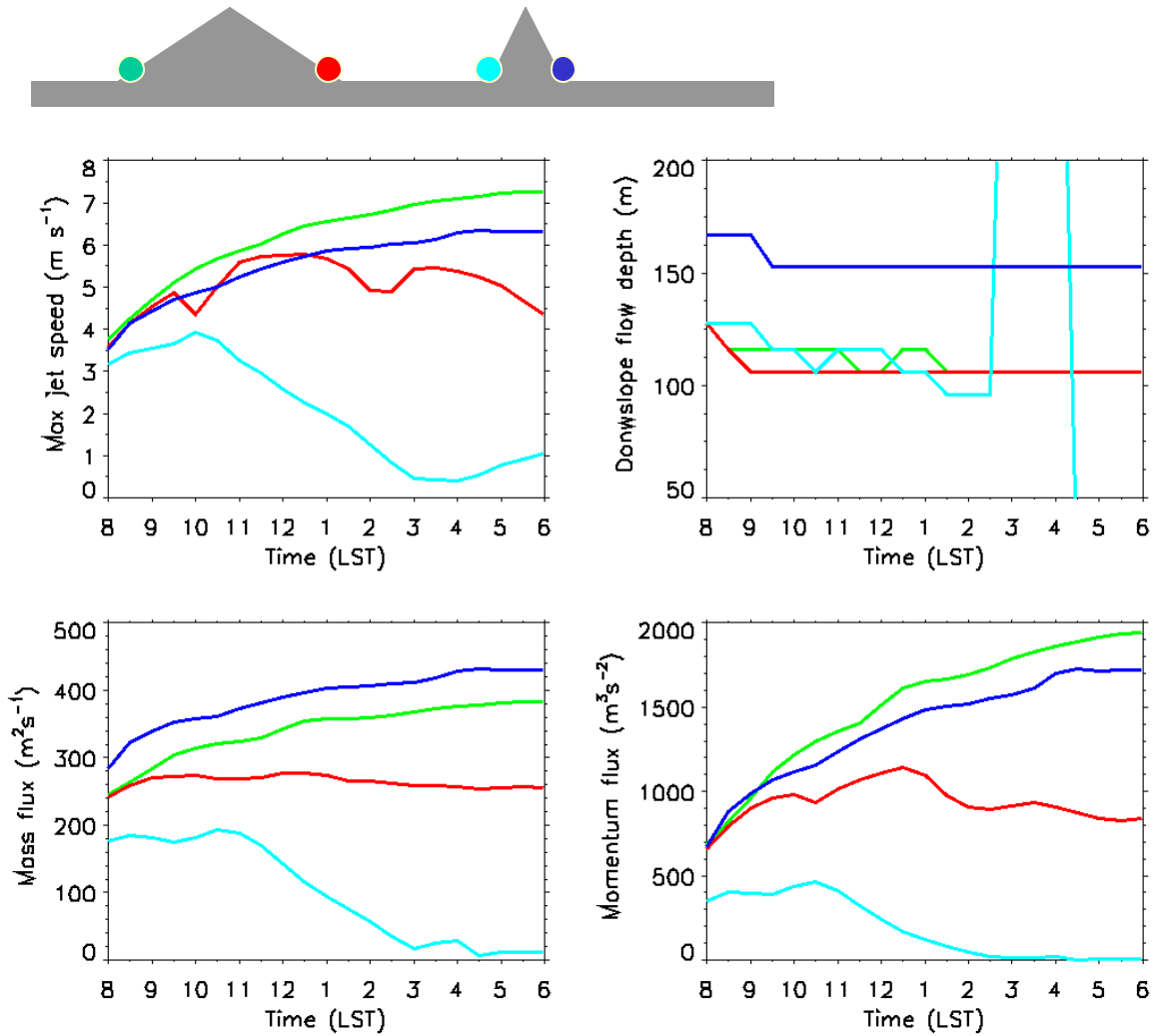


Fig. 6. Time series of the maximum drainage wind speed, depth of the drainage flow, and the mass and momentum fluxes from the simulation of Oct. 2 at a point on each side of the four slopes near the bottom of the slopes